Dark Energy - Dark Matter Unification:
Generalized Chaplygin Gas Model

- Type Ia Supernovae and Accelerated Expansion
- Quintessence
- Quintessence and the Brane
- Generalized Chaplygin Gas Model

CMBR Constraints

Supernovae and Gravitational Lensing Constraints

Structure Formation

M.C. Bento, O. B., A.A. Sen
Phys. Rev. D66 (2002) 043507; D67 (2003) 063003; D70 (2004) 083519
Phys. Lett. B575 (2003) 172; Gen. Rel. Grav. 35 (2003) 2063

O. B., A.A. Sen, S. Sen, P.T. Silva
Mon. Not. Roy. Astron. Soc. 353 (2004) 329

P.T. Silva, O. B.
Astrophys. J. 599 (2003) 829

O. B.
astro-ph/0403310; astro-ph/0504275

M.C. Bento, O. B., N.M. Santos, A.A. Sen
Phys. Rev. D71 (2005) 063501

Orfeu Bertolami
Instituto Superior Técnico, Depto. Física, Lisbon

KIAS-APCTP-DMRC Workshop on ”The Dark Side of the Universe”
24-26 May, 2005, KIAS, Seoul, Korea

Type Ia Supernovae and Accelerated Expansion

Study of recently discovered Type Ia Supernovae with $z \geq 0.35$ indicates that the deceleration parameter

$$q_0 \equiv -\frac{\ddot{a}\, a}{\dot{a}^2} \; ,$$

where $a(t)$ is the scale factor, is negative

$$-1 \lesssim q_0 < 0 \; .$$

[Permutter et al. 1998; Riess et al. 1999]

For an homogeneous and isotropic expanding geometry driven by the vacuum energy, Ω_V and matter Ω_M with Eqs. of state of the form

$$p = \omega\rho \qquad -1 \leq \omega \leq 1 \quad ,$$

it follows from the Friedmann and Raychaudhuri Eqs.

$$q_0 = \frac{1}{2}(3\omega + 1)\Omega_M - \Omega_\Lambda \quad .$$

A negative q_0 suggests that a dark energy, an “invisible” smoothly distributed energy density, is the dominant component. This energy density can have its origin either on a non-vanishing cosmological constant, Λ, or on a dynamical vacuum energy, “quintessence”, Ω_Q $(\omega_Q < -1/3)$.

Cosmological Constraints

Observational Parameters

$$\Omega_M \simeq 0.30$$

$$\Omega_{\Lambda,Q} \simeq 0.70$$

$$\Omega_k \simeq 0$$

$$H_0 = 100\, h\; km\; s^{-1}\; Mpc^{-1} \;\;,\;\; h = 0.71$$

Big-Bang Nucleosynthesis (BBN)

$$V(\phi) = V_0 \exp\left(-\lambda\phi\right)$$

$$\Omega_\phi < 0.045\,(2\,\sigma) \;\;\Rightarrow\;\; \lambda > 9$$

[Bean, Hansen, Melchiorri 2001]

Cosmic Microwave Background

$$\omega_\phi < -0.6\,(2\,\sigma) \qquad \textit{Flat models}$$

$$\Omega_\phi < 0.39\,(2\,\sigma) \;\;\Rightarrow\;\; \lambda \gtrsim 6$$

[Efstathiou 1999]

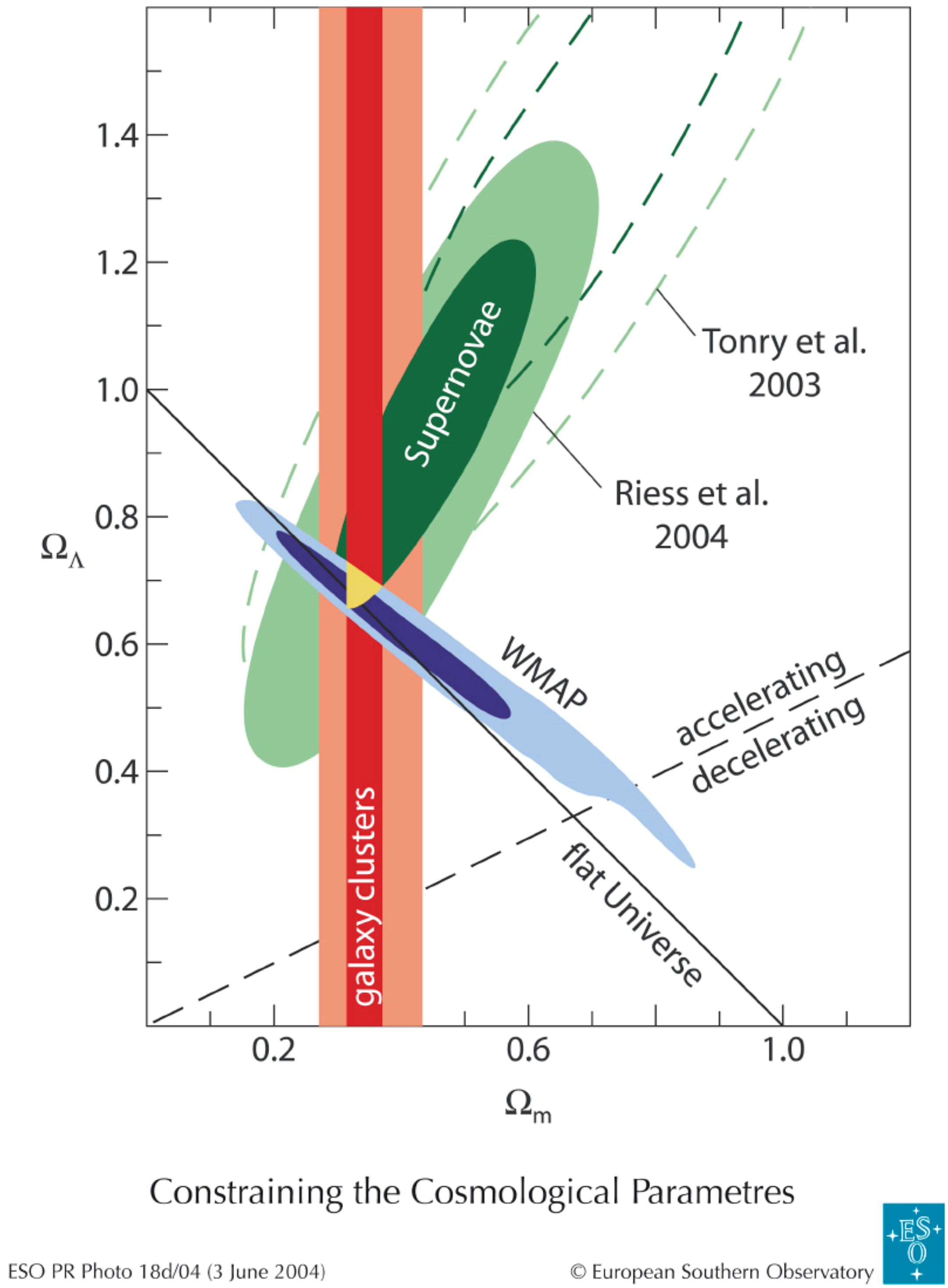

Figure 1: Concordance Model (latest)

Some Ideas

- $V_0 \exp(-\lambda\phi)$ (Troublesome on the brane)

[Ratra, Peebles 1988; Wetterich 1988; Ferreira, Joyce 1998]

- $V_0\phi^{-\alpha}\ ,\ \alpha > 0$ (Fine on the brane for $2 < \alpha < 6$)

[Ratra, Peebles 1988]

- $V_0\,\phi^{-\alpha}\ \exp(\lambda\phi^2)\ ,\ \alpha > 0$ [Brax, Martin 1999, 2000]

- $V_0\left[\exp(M_p/\phi) - 1\right]$ [Zlatev, Wang, Steinhardt 1999]

- $V_0(\cosh\lambda\phi - 1)^p$ [Sahni, Wang 2000]

- $V_0\sinh^{-\alpha}(\lambda\phi)$

[Sahni, Starobinsky 2000; Ureña-López, Matos 2000]

- $V_0[\exp(\beta\phi) + \exp(\gamma\phi)]$ [Barreiro, Copeland, Nunes 2000]

- Scalar-Tensor Theories of Gravity

[Uzan 1999; Amendola 1999; O.B., Martins 2000; Fujii 2000; ...]

- $V_0\exp(-\lambda\phi)[A + (\phi - B)^2]$ [Albrecht, Skordis 2000]

- $V_0\exp(-\lambda\phi)[a + (\phi-\phi_0)^2 + b\,(\psi-\psi_0)^2 + c\,\phi(\psi-\psi_0)^2 + d\,\psi(\phi-\phi_0)^2]$

[Bento, O.B., Santos 2002]

Quintessence and the Brane

Brane-World Scenarios

[L. Randall, R. Sundrum 1999, ...]

- 5-dim AdS spacetime in the bulk with matter confined on a 3-brane $\Rightarrow$ 4-dimensional Einstein Eqs.

$$G_{\mu\nu} = -\Lambda g_{\mu\nu} + \frac{8\pi}{M_P^2} T_{\mu\nu} + \left(\frac{8\pi}{M_5^3}\right)^2 S_{\mu\nu} - E_{\mu\nu} \ .$$

[Shiromizu, Maeda, Sasaki 2000]

If $T_{\mu\nu}$ is the energy-momentum of a perfect fluid on the brane, then

$$S_{\mu\nu} = \frac{1}{2}\rho^2 u_\mu u_\nu + \frac{1}{12}\rho(\rho + 2p) h_{\mu\nu} \ ,$$

ρ, p are the energy density and isotropic pressure of a fluid with 4-velocity u_μ, $h_{\mu\nu} = g_{\mu\nu} + u_\mu u_\nu$,

$$E_{\mu\nu} = -\frac{6}{k^2\lambda}[\epsilon(u_\mu u_\nu + \frac{1}{3}h_{\mu\nu}) + P_{\mu\nu} + Q_\mu u_\nu + Q_\nu u_\mu] \ ,$$

so that $k^2 \equiv 8\pi/M_P^2$ (GR limit $\lambda^{-1} \to 0$) and the tensors $P_{\mu\nu}$ and Q_μ correspond to non-local contributions to pressure and flux of energy. For a perfect fluid $P_{\mu\nu} = Q_\mu = 0$ and $\epsilon = \epsilon_0 a^{-4}$.

The 4-dimensional cosmological constant is related to the 5-dimensional one and the 3-brane tension, λ:

$$\Lambda = \frac{4\pi}{M_5^3}\left(\Lambda_5 + \frac{4\pi}{3M_5^3}\lambda^2\right)$$

while the Planck scale is given by

$$M_P = \sqrt{\frac{3}{4\pi}\frac{M_5^3}{\sqrt{\lambda}}} \ .$$

In a cosmological setting, where the 3-brane resembles our Universe and the metric projected onto the brane is an homogeneous and isotropic flat Robertson-Walker metric, the generalized Friedmann Eq. reads

$$H^2 = \frac{\Lambda}{3} + \left(\frac{8\pi}{3M_P^2}\right)\rho + \left(\frac{4\pi}{3M_5^3}\right)\rho^2 + \frac{\epsilon_0}{a^4} \quad .$$

[Binétruy, Deffayet, Ellwanger, Langlois 2000]
[Flanagan, Tye, Wasserman 2000]

Choosing $\Lambda_5 \simeq -4\pi\lambda^2/3M_5^3$ and dropping the term $\epsilon_0 a^{-4}$ which quickly vanishes after inflation:

$$H^2 = \frac{8\pi}{3M_P^2}\rho\left[1 + \frac{\rho}{2\lambda}\right] \quad .$$

Extra brane term:
Beneficial for some quintessence models, but harmful for some others!

[Mizuno, Maeda 2001]

Generalized Chaplygin Gas

• Radical new idea: change of behaviour of the missing energy density might be controlled by the change in the equation of state of the background fluid.

• Interesting case: Chaplygin gas, described by the Eq. of state

$$p = -\frac{A}{\rho^\alpha} \ ,$$

with $\alpha = 1$ and A a positive constant.

• From the relativistic energy conservation Eq., within the framework of a Friedmann-Robertson-Walker cosmology,

$$\rho = \sqrt{A + \frac{B}{a^6}} \ ,$$

where B is an integration constant.

• Smooth interpolation between a dust dominated phase where, $\rho \simeq \sqrt{B} a^{-3}$, and a De Sitter phase where $p \simeq -\rho$, through an intermediate regime described by the equation of state for "stiff" matter, $p = \rho$.

[Kamenshchik, Moschella, Pasquier 2001]

This setup admits a brane interpretation via a parametrization invariant Nambu-Goto d-brane action in a $(d+1, 1)$ spacetime. This action leads, in the light-cone parametrization, to the Poincaré-invariant Born-Infeld action in a $(d, 1)$ spacetime. The Chaplygin is the only known gas to admit a supersymmetric generalization.

[Jackiw 2000]

• Bearing on the observed accelerated expansion of the Universe: Eq. of state is asymptotically dominated by a cosmological constant, $8\pi G\sqrt{A}$.

• Inhomogeneous generalization can be regarded as a dark energy - dark matter unification.

[Bilić, Tupper, Viollier 2001]
[Bento, O.B., Sen 2002]

A Model ($0 < \alpha \leq 1$)

- Lagrangian density for a massive complex scalar field, Φ:

$$\mathcal{L} = g^{\mu\nu}\Phi^*_{,\mu}\Phi_{,\nu} - V(|\Phi|^2) \ .$$

Writing $\Phi = (\frac{\phi}{\sqrt{2}m})\exp(-im\theta)$ in terms of its mass, m:

$$\mathcal{L} = \frac{1}{2}g^{\mu\nu}\left(\phi^2\theta_{,\mu}\theta_{,\nu} + \frac{1}{m^2}\phi_{,\mu}\phi_{,\nu}\right) - V(\phi^2/2) \ .$$

Scale of inhomogeneities arises from the assumption:

$$\phi_{,\mu} << m\phi \ .$$

- Lagrangian density in this "Thomas-Fermi" approximation:

$$\mathcal{L}_{TF} = \frac{\phi^2}{2}g^{\mu\nu}\theta_{,\mu}\theta_{,\nu} - V(\phi^2/2) \ .$$

- Equations of motion:

$$g^{\mu\nu}\theta_{,\mu}\theta_{,\nu} = V'(\phi^2/2) \ ,$$

$$(\phi^2\sqrt{-g}g^{\mu\nu}\theta_{,\nu})_{,\mu} = 0 \ ,$$

where $V'(x) \equiv dV/dx$. Phase θ can be regarded as a velocity field whether $V' > 0$, that is

$$U^\mu = \frac{g^{\mu\nu}\theta_{,\nu}}{\sqrt{V'}} \ ,$$

so that, on the mass shell, $U^\mu U_\mu = 1$.

- Energy-momentum tensor takes the form of a perfect fluid:

$$\rho = \frac{\phi^2}{2}V' + V \ ,$$

$$p = \frac{\phi^2}{2}V' - V \ .$$

• Covariant conservation of the energy-momentum tensor

$$\dot{\rho} + 3H(p+\rho) = 0 \ ,$$

where $H = \dot{a}/a$, leads for the generalized Chaplygin gas

$$\rho = \left(A + \frac{B}{a^{3(1+\alpha)}}\right)^{\frac{1}{1+\alpha}} \ .$$

Furthermore

$$d \ \ln\phi^2 = \frac{d(\rho - p)}{\rho + p} \ ,$$

which, together with the Eq. of state implies that:

$$\phi^2(\rho) = \rho^\alpha(\rho^{1+\alpha} - A)^{\frac{1-\alpha}{1+\alpha}} \ .$$

• Generalized Born-Infeld theory:

$$\mathcal{L}_{GBI} = -A^{\frac{1}{1+\alpha}}\left[1 - (g^{\mu\nu}\theta_{,\mu}\theta_{,\nu})^{\frac{1+\alpha}{2\alpha}}\right]^{\frac{\alpha}{1+\alpha}} \ ,$$

which reproduces the Born-Infeld Lagrangian density for $\alpha = 1$.

• $\mathcal{L}_{GBI}$ can be regarded as a d-brane plus soft correcting terms as can be seen from the expansion around $\alpha = 1$:

$$\left[1 - X^{\frac{1+\alpha}{2\alpha}}\right]^{\frac{\alpha}{1+\alpha}} = \sqrt{1-X} + \frac{X\log(X) + (1-X)\log(1-X)}{4\sqrt{1-X}}(1-\alpha)$$
$$+\frac{E+F+G}{32(1-X)^{3/2}}(1-\alpha)^2 + \mathcal{O}((1-\alpha)^3) \ ,$$

where $X \equiv g^{\mu\nu}\theta_{,\mu}\theta_{,\nu}$ and

$$E = X(X-2)\log^2(X) \ ,$$

$$F = -2X(X-1)\log(X)[\log(1-X) - 2] \ ,$$

$$G = (X-1)^2[\log(1-X) - 4]\log(1-X) \ .$$

• Potential arising from the model

$$V = \frac{\rho^{1+\alpha} + A}{2\rho^{\alpha}} = \frac{1}{2}\left(\Psi^{2/\alpha} + \frac{A}{\Psi^2}\right) \quad ,$$

where $\Psi \equiv B^{-(1-\alpha/1+\alpha)} a^{3(1-\alpha)} \phi^2$, which reduces to the duality invariant, $\phi^2 \rightarrow A/\phi^2$, and scale-factor independent potential for the Chaplygin gas.

• Intermediate regime between the dust dominated phase and the De Sitter phase:

$$\rho \simeq A^{\frac{1}{1+\alpha}} + \left(\frac{1}{1+\alpha}\right) \frac{B}{A^{\frac{\alpha}{1+\alpha}}} a^{-3(1+\alpha)} \quad ,$$

$$p \simeq -A^{\frac{1}{1+\alpha}} + \left(\frac{\alpha}{1+\alpha}\right) \frac{B}{A^{\frac{\alpha}{1+\alpha}}} a^{-3(1+\alpha)} \quad ,$$

which corresponds to a mixture of vacuum energy density $A^{\frac{1}{1+\alpha}}$ and matter described by the “soft” equation of state:

$$p = \alpha\rho \quad .$$

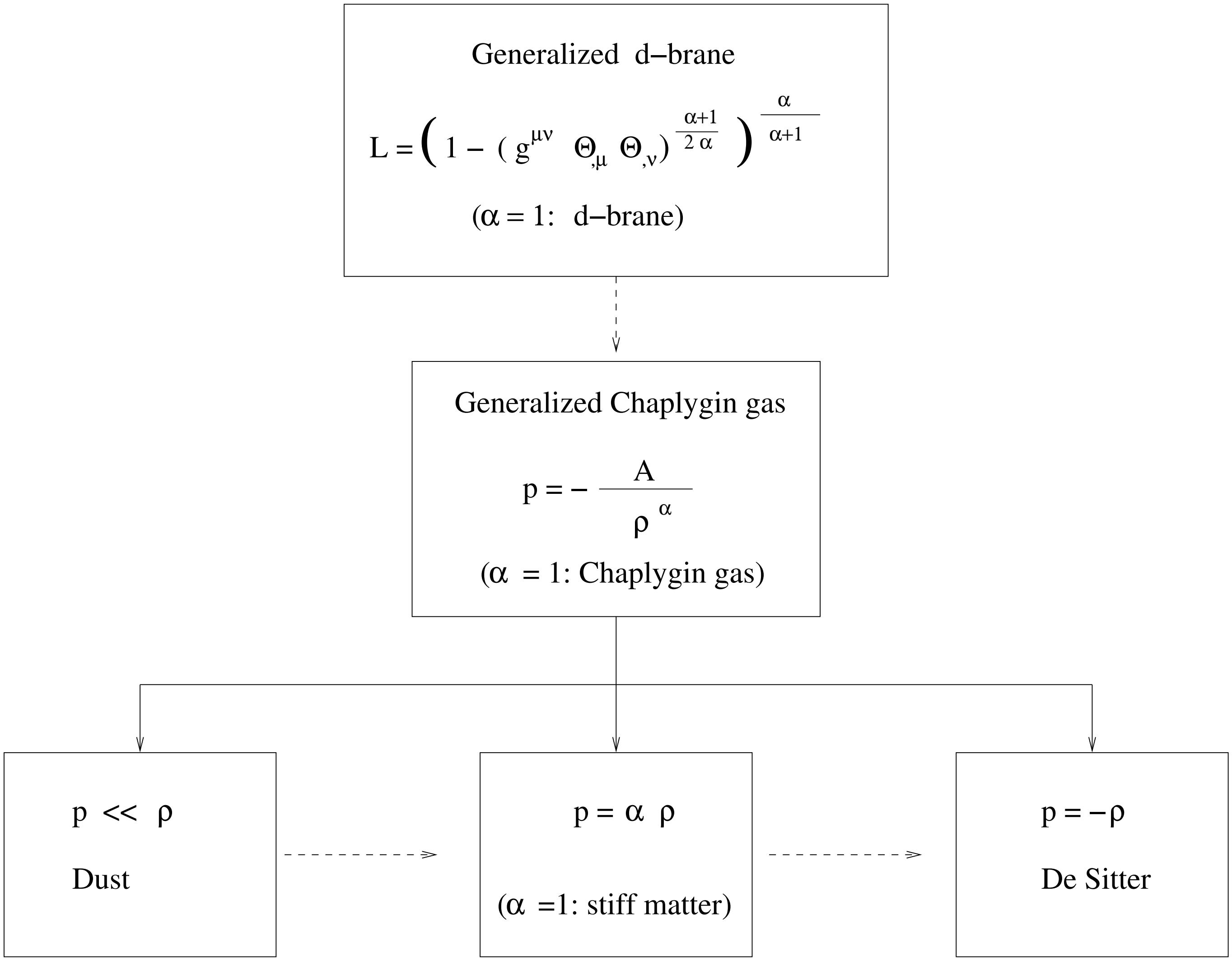

Figure 2: Cosmological evolution of a universe described by a generalized Chaplygin gas equation of state.

Treatment of the Inhomogeneities

• Second equation of motion admits as first integral a position dependent function $B(\vec{r})$, after a convenient choice of comoving coordinates where the velocity field is given by $U^{\mu} = \delta_0^{\mu}/\sqrt{g_{00}}$. An induced induced 3-metric

$$\gamma_{ij} = \frac{g_{i0}g_{j0}}{g_{00}} - g_{ij}$$

with determinant $\gamma \equiv -g/g_{00}$ can be built after choosing the proper time, $d\tau = \sqrt{g_{00}}dx^0$.

For the relevant scales, function $B(\vec{r})$ can be regarded as approximately constant, hence

$$\rho = \left(A + \frac{B}{\gamma^{(1+\alpha)}} \right)^{\frac{1}{1+\alpha}} \quad .$$

Zeldovich method for considering inhomogeneities can be implemented through the deformation tensor:

$$D_{ij} = a(t) \left(\delta_{ij} - b(t) \frac{\partial^2 \varphi(\vec{q})}{\partial q^i \partial q^j} \right) \quad ,$$

where $\vec{q}$ are generalized Lagrangian coordinates and

$$\gamma_{ij} = \delta_{mn} D_i^m D_j^n \quad ,$$

h being a perturbation

$$h = 2b(t) \varphi_{,i}{}^{i} \quad ,$$

with $b(t)$ parametrizing the time evolution of the inhomogeneities and

$$\rho \simeq \bar{\rho}(1+\delta) \quad , \quad p \simeq -\frac{A}{\bar{\rho}^{\alpha}}(1-\alpha\delta) \quad ,$$

$\bar{\rho}$ being given by the evolution Eq. of the energy density and the density contrast, δ, by

$$\delta = \frac{h}{2}(1+w) \quad ,$$

with

$$w \equiv \frac{p}{\rho} = -\frac{A}{\bar{\rho}^{1+\alpha}} \quad .$$

The induced metric leads to the $(0-0)$ component of the Einstein Eqs:

$$-3\frac{\ddot{a}}{a} + \frac{1}{2}\ddot{h} + H\dot{h} = 4\pi G \bar{\rho}[(1+3w) + (1-3\alpha w)\delta] \quad ,$$

where the unperturbed part corresponds to the Raychaudhuri Eq.

$$-3\frac{\ddot{a}}{a} = 4\pi G \bar{\rho}(1+3w) \quad .$$

It follows from the Friedmann Eq. for a flat space section

$$H^2 = \frac{8\pi G}{3}\bar{\rho} \ ,$$

that the Einstein's Eqs. can be written as a differential equation for $b(a)$:

$$\frac{2}{3}a^2 b'' + (1-w)ab' - (1+w)(1-3\alpha w)b = 0 \ ,$$

where the primes denote derivatives with respect to the scale-factor. From the observational constraints

$$w(a) = -\frac{\Omega_\Lambda a^{3(1+\alpha)}}{1-\Omega_\Lambda + \Omega_\Lambda a^{3(1+\alpha)}} \ .$$

•We numerically integrate the Eq. for b for different values of α using $a_{eq} = 10^{-4}$ for matter-radiation equilibrium, $a_0 = 1$ at present and $b'(a_{eq}) = 0$ as initial condition.

• Generalized Chaplygin scenarios start differing from the ΛCDM only recently ($z \lesssim 1$) and yield a density contrast that closely resembles, for any value of $\alpha \neq 0$, the standard CDM before the present.

It can be seen that for any value of α, $b(a)$ saturates as in the ΛCDM.

• Ratio between δ in the Chaplygin and the ΛCDM scenarios is given by:

$$\frac{\delta_{Chap}}{\delta_{\Lambda CDM}} = \frac{b_{Chap}}{b_{\Lambda CDM}} \frac{1 - \Omega_\Lambda + \Omega_\Lambda a^3}{1 - \Omega_\Lambda + \Omega_\Lambda a^{3(1+\alpha)}} \ ,$$

meaning that their difference diminishes as a evolves.

Evolution of δ as a function of a can be obtained from numerical integration. We find that for any value of α the density contrast decays for large a (as the $\alpha = 1$ case).

[Bilić, Tupper, Viollier 2001]

[Fabris, Gonçalves, Souza 2001]

The difference in behaviour of the density contrast between a Universe filled with matter with a "soft" or "stiff" Eqs. of state can be seen in the Figure. The former resembles more closely the ΛCDM.

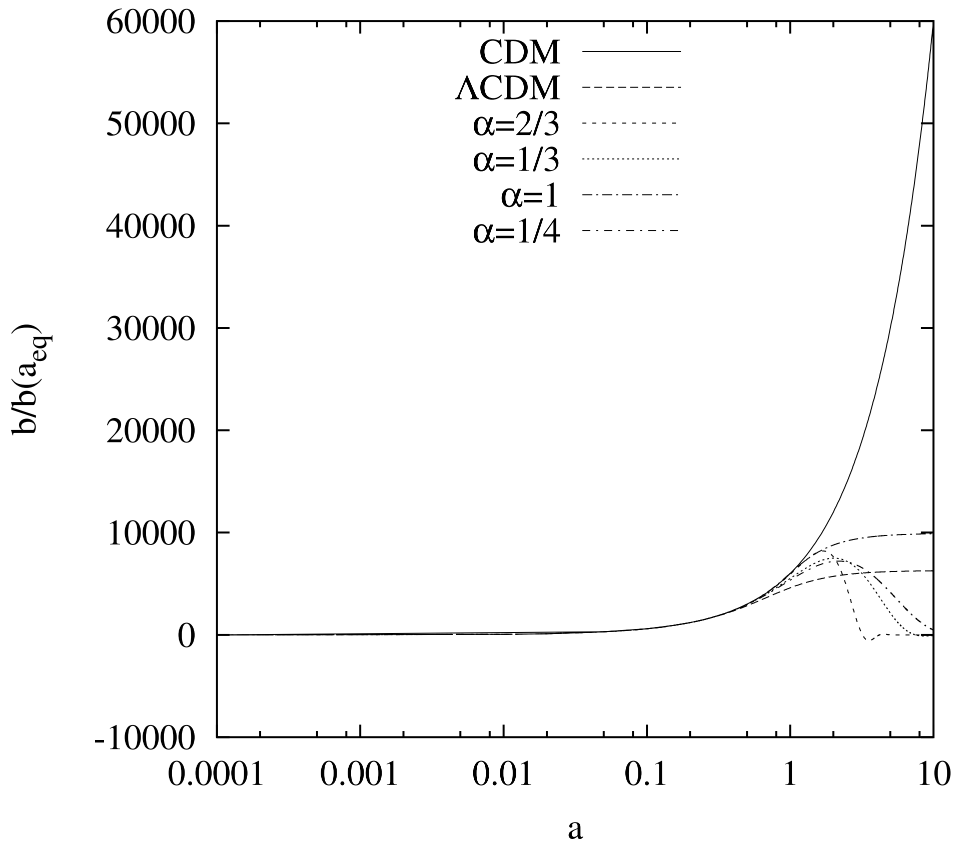

Figure 3: Evolution of $b(a)/b(a_{eq})$ for the generalized Chaplygin gas model, for different values of α, as compared with CDM and ΛCDM.

Location of CMBR peaks for the generalized Chaplygin gas

• CMBR peaks arise from acoustic oscillations of the primeval plasma just before the Universe becomes transparent. The angular momentum scale of the oscillations is set by the acoustic scale l_A, which for a flat Universe is given by

$$l_A = \pi \frac{\tau_0 - \tau_{\rm ls}}{\bar{c}_s \tau_{\rm ls}} \quad ,$$

where τ_0 and $\tau_{\rm ls}$ are the conformal time at present and at the last scattering and $\bar{c}_s$ is the average sound speed before decoupling.

The assumptions in our subsequent calculations are as follows:
Scale factor at present $a_0 = 1$, scale factor at last scattering $a_{ls} = 1100^{-1}$, $h = 0.65$, density parameter for radiation and baryons at present $\Omega_{r0} = 9.89 \times 10^{-5}$, $\Omega_{b0} = 0.05$, average sound velocity $\bar{c}_s = 0.52$, and spectral index for the initial energy density perturbations, $n = 1$.
To compute l_A we rewrite the Chaplygin equation in the form

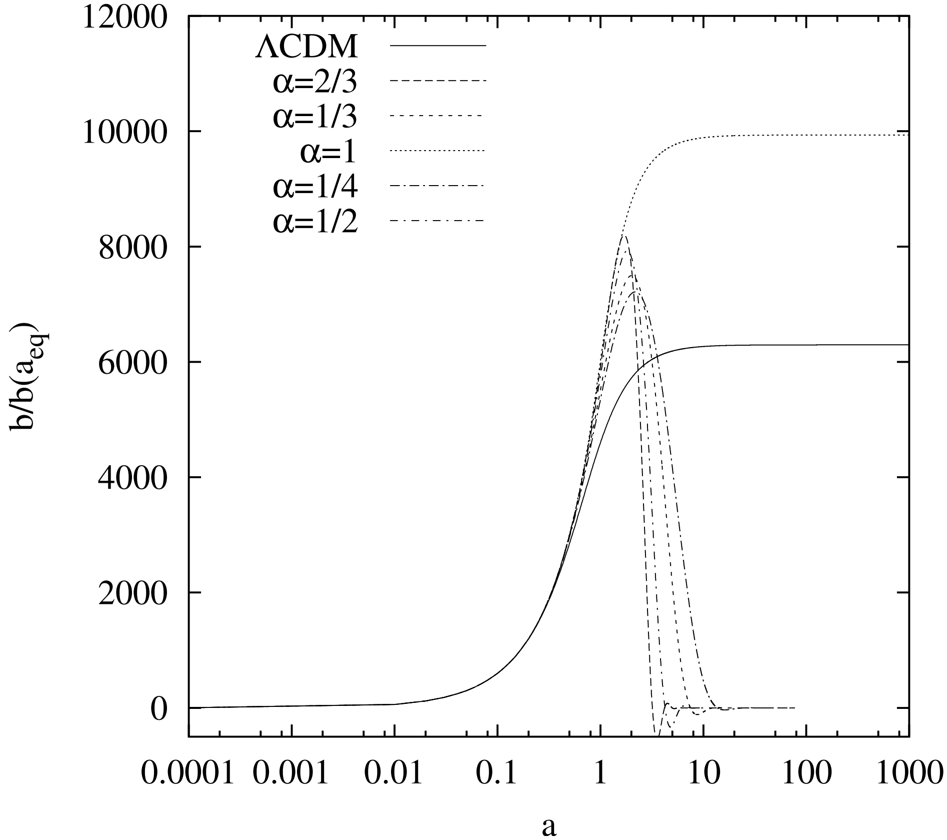

Figure 4: Evolution of $b(a)/b(a_{eq})$ for the generalized Chaplygin gas model, for different values of α, as compared with ΛCDM.

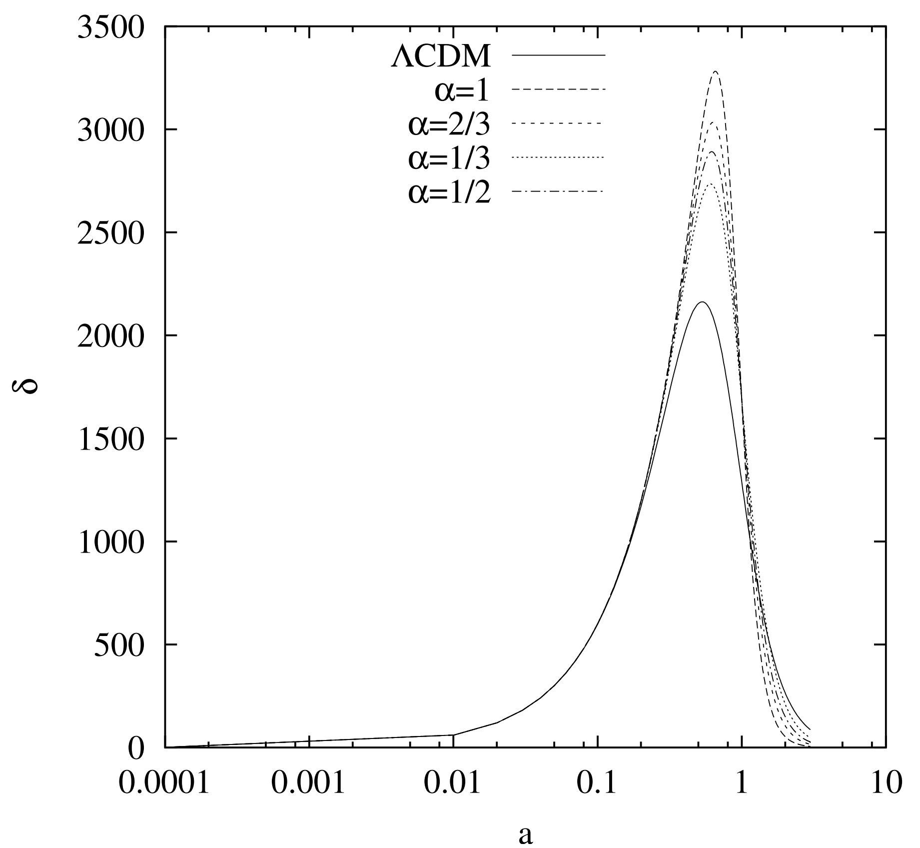

Figure 5: Density contrast for different values of α, as compared with $b\Lambda$CDM.

$$\rho_{ch} = \rho_{ch0}\left(A_s + \frac{(1-A_s)}{a^{3(1+\alpha)}}\right)^{1/1+\alpha} \quad ,$$

where $A_s \equiv A/\rho_{ch0}^{1+\alpha}$ and $\rho_{ch0} = (A+B)^{1/1+\alpha}$. The Friedmann eq. becomes

$$H^2 = \frac{8\pi G}{3}\left[\frac{\rho_{r0}}{a^4} + \frac{\rho_{b0}}{a^3} + \rho_{ch0}\left(A_s + \frac{(1-A_s)}{a^{3(1+\alpha)}}\right)^{1/1+\alpha}\right] \quad ,$$

where we have included the contribution of radiation and baryons.
Several important features are worth remarking:
(i) $0 \leq A_s \leq 1$ (ii) For $A_s = 0$ the Chaplygin gas behaves as dust and, for $A_s = 1$, it behaves like as a cosmological constant. For $\alpha = 0$, the Chaplygin gas corresponds to a ΛCDM model. Hence, for the chosen range of α, the generalised Chaplygin gas is clearly different from ΛCDM. Another relevant issue is that the sound velocity of the fluid is given, at present, by αA_s and thus $\alpha A_s \leq 1$. Moreover using that

$$\frac{\rho_{r0}}{\rho_{ch0}} = \frac{\Omega_{r0}}{\Omega_{ch0}} = \frac{\Omega_{r0}}{1-\Omega_{r0}-\Omega_{b0}},$$

and

$$\frac{\rho_{b0}}{\rho_{ch0}} = \frac{\Omega_{b0}}{\Omega_{ch0}} = \frac{\Omega_{b0}}{1-\Omega_{r0}-\Omega_{b0}},$$

we obtain

$$H^2 = \Omega_{ch0} H_0^2 a^{-4} X^2(a) \quad ,$$

with

$$X(a) = \frac{\Omega_{r0}}{1-\Omega_{r0}-\Omega_{b0}} + \frac{\Omega_{b0}\, a}{1-\Omega_{r0}-\Omega_{b0}} + a^4\left(A_s + \frac{(1-A_s)}{a^{3(1+\alpha)}}\right)^{1/1+\alpha} \quad .$$

From the fact that $H^2 = a^{-4}\left(\frac{da}{d\tau}\right)^2$, we get

$$d\tau = \frac{da}{\Omega_{ch0}^{1/2} H_0 X(a)} \quad ,$$

so that

$$l_A = \frac{\pi}{\bar{c}_s}\left[\int_0^1 \frac{da}{X(a)}\left(\int_0^{a_{ls}} \frac{da}{X(a)}\right)^{-1} - 1\right] \ .$$

In an idealised model of the primeval plasma, there is a simple relation between the location of the m-th peak and the acoustic scale, namely $l_m \approx m l_A$. However, the location of the peaks is slightly shifted by driving effects and this can be compensated by parameterising the location of the m-th peak, l_m as

$$l_m \equiv l_A\left(m - \varphi_m\right) \ .$$

It is not possible in general to analytically derive a relationship between the cosmological parameters and the peak shifts, but one can use fitting formulae. In particular, for $n = 1$ and $\Omega_{b0}h^2 = 0.02$ one finds that:

$$\varphi_1 \approx 0.267\left(\frac{r_{ls}}{0.3}\right)^{0.1} \ ,$$

where $r_{ls} = \rho_r(z_{ls})/\rho_m(z_{ls})$.

[Doran, Lilley, Schwindt, Wetterich 2000]

[Hu, Fukugita, Zaldarriaga, Tegmark 2001]

According to the dark energy - dark matter unification hypothesis, ρ_{ch} will behave as non-relativistic matter at the last scattering and hence

$$\rho_{ch} \approx \frac{\rho_{ch0}}{a^3}(1 - A_s)^{1/1+\alpha} \ ,$$

from which follows

$$r_{ls} = \frac{\Omega_{r0}}{\Omega_{ch0}}\frac{a_{ls}^{-1}}{(1 - A_s)^{1/1+\alpha}} \simeq \frac{\Omega_{r0}a_{ls}^{-1}}{(1 - \Omega_{r0} - \Omega_{b0})(1 - A_s)^{1/1+\alpha}} \ .$$

We show l_1 as a function of α for different values of A_s, for the observational bounds on l_1 as derived from BOOMERANG (dashed lines)

$$l_1 = 221 \pm 14 \quad .$$

and Archeops data (full lines)

$$l_1 = 220 \pm 6 \quad .$$

Notice that, since $\alpha A_s \leq 1$, for a specific value of A_s curves end where this relation gets saturated, $\alpha A_s = 1$.

• It is very difficult to extract any constraints from the position of the second peak since it depends on too many parameters, hence it is disregarded. As for the shift of the third peak, it turns out to be a relatively insensitive quantity

$$\varphi_3 \approx 0.341 \quad .$$

[Doran, Lilley, Wetterich 2001]

We show l_3 as a function of α for different values of A_s, in relation to the current lower and upper bounds on l_3 as derived from BOOMERANG data

$$l_3 = 825^{+10}_{-13} \quad .$$

We see that l_1 and l_3 put rather tight constraints on the parameters of the model, α and A_s.

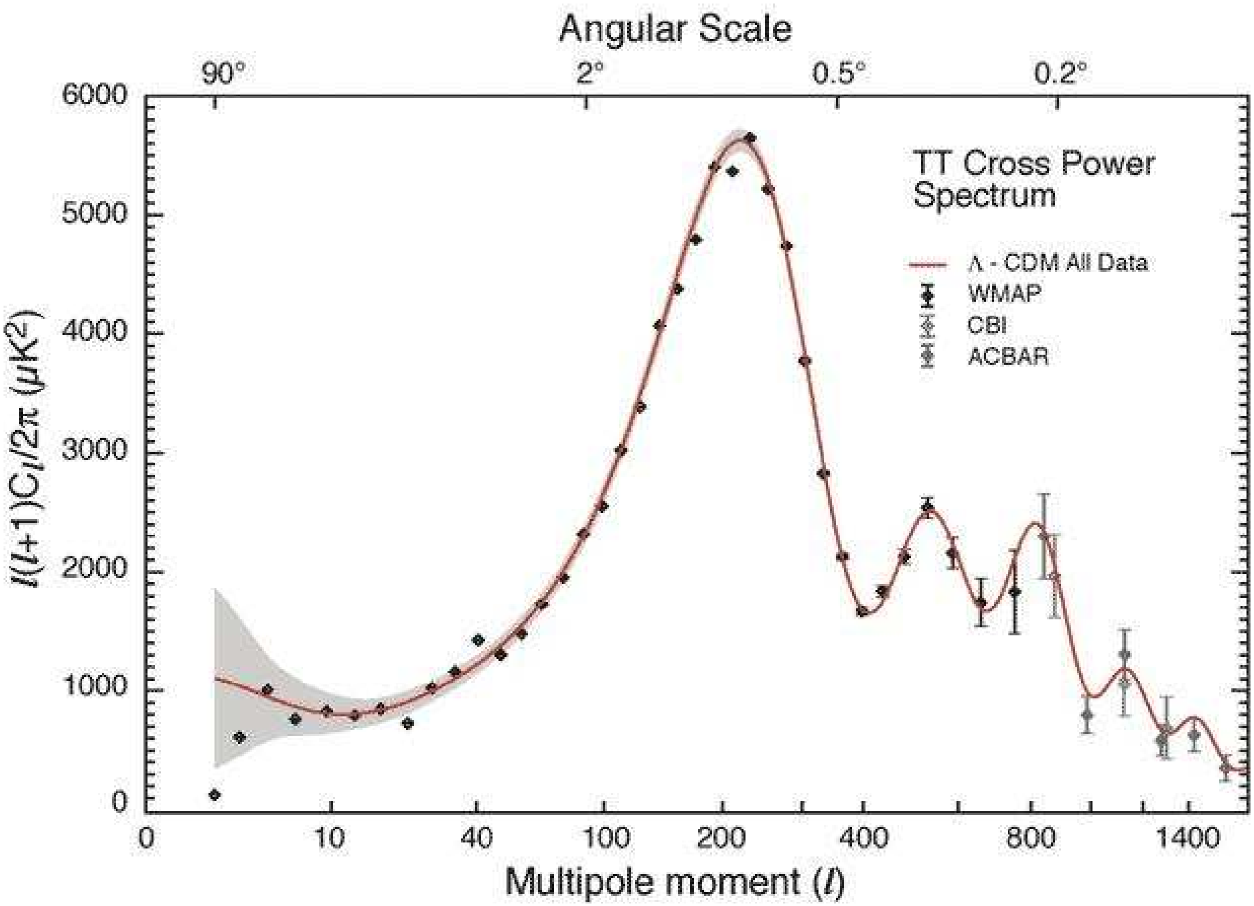

Figure 6: WMAP Power Spectrum

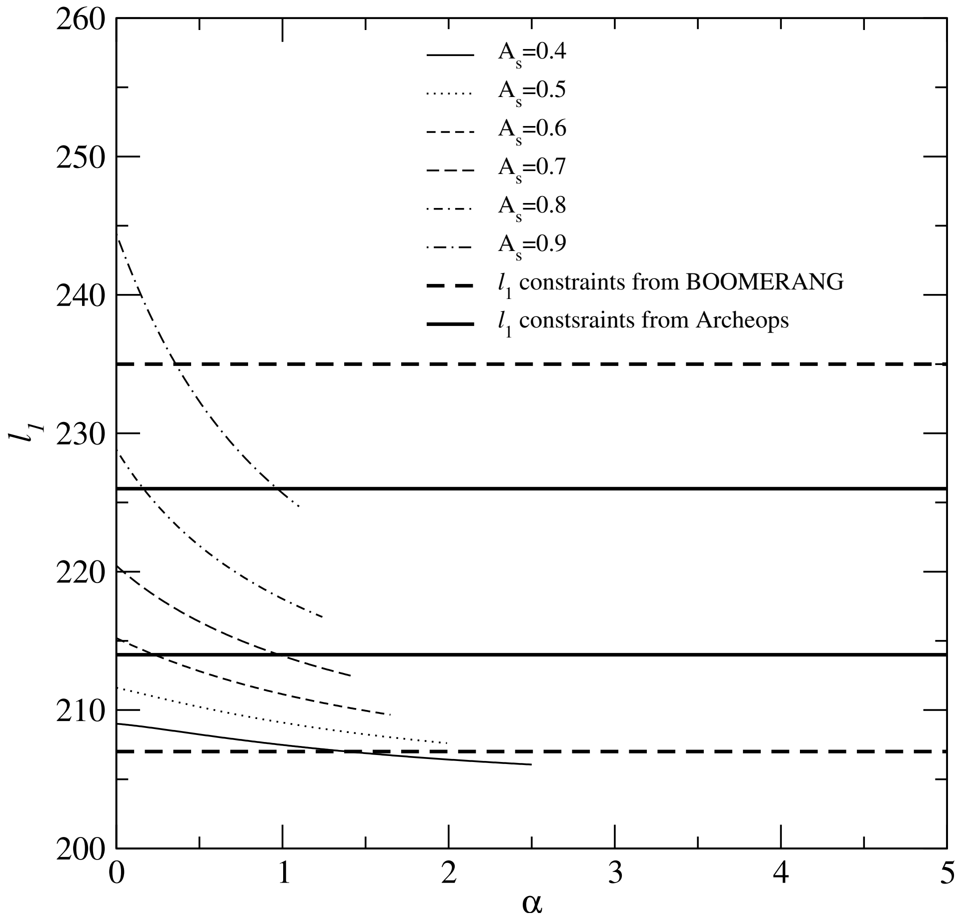

Figure 7: Dependence of the position of the CMBR first peak, l_1, as a function of α for different values of A_S. Also shown are the observational bounds on l_1 from BOOMERANG (dashed lines), and Archeops (full lines).

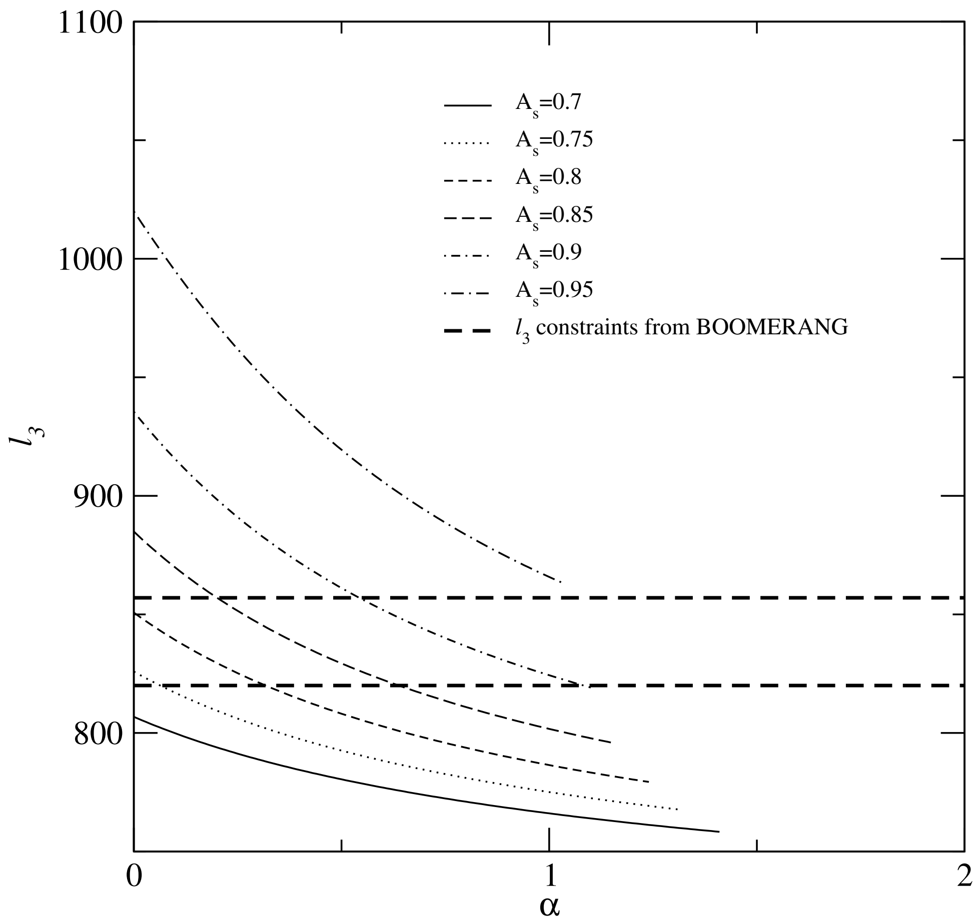

Figure 8: Dependence of the position of the CMBR third peak, l_3, as a function of α for different values of A_S. Also shown are the observational bounds on l_3 (dashed lines).

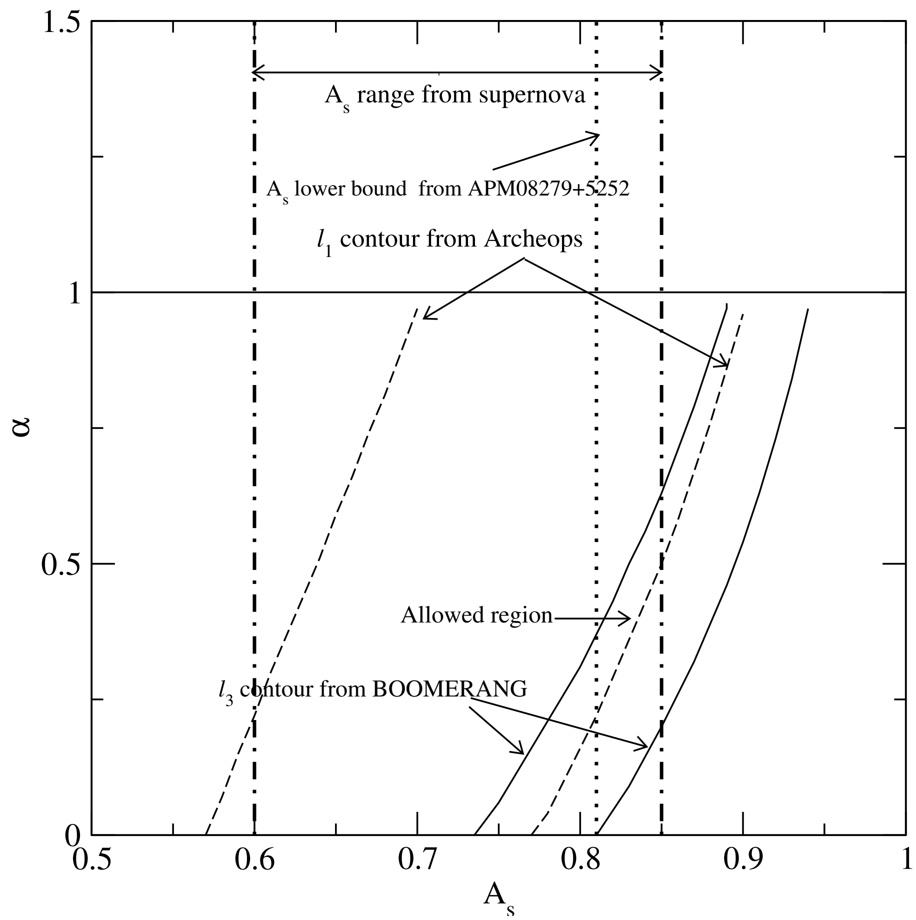

Figure 9: Contours in the (α, A_S) plane arising from Archeops constraints on l_1 (full contour) and BOOMERANG constraints on l_3 (dashed contour), supernova and APM $08279 + 5255$ object. The allowed region of the model parameters lies in the intersection between these regions.

WMAP Constraints

$$l_1 = 220.1 \pm 0.8 \quad l_2 = 546 \pm 10 \quad l_{d1} = 411.7 \pm 3.5$$

Main conclusions:

1. Assuming WMAP priors, the Chaplygin gas model, $\alpha = 1$, is incompatible with the data and so are models with $\alpha \gtrsim 0.6$

2. For $\alpha = 0.6$, consistency with data requires for the spectral tilt, $n_s > 0.97$, and that, $h \lesssim 0.68$

3. The ΛCDM model barely fits the data for $n_s \simeq 1$ (WMAP data yields $n_s = 0.99 \pm 0.04$) and for that $h > 0.72$. For low values of n_s, ΛCDM is preferred to the GCG models. For intermediate values of n_s, the GCG model is favoured only if $\alpha \simeq 0.2$

These results are consistent with the ones obtained by Amendola et al. 2003 using the CMBFast code. Furthermore, we find:

4. In the (A_s, α) plane the variation of h within the bounds $h = 0.71^{+0.04}_{-0.03}$ does not lead to important changes in the allowed regions, as compared to the value $h = 0.71$. However, these regions become slightly larger as they shift up-wards for $h < 0.71$; the opposite trend is found for $h > 0.71$

5. Our results are consistent with bounds obtained using BOOMERanG data for the third peak and Archeops data for the first peak as well as results from SNe Ia and age bounds, namely $0.81 \lesssim A_s \lesssim 0.85$ and $0.2 \lesssim \alpha \lesssim 0.6$

6. If one abandons the constraint on h arising from WMAP, then the Chaplygin gas case $\alpha = 1$ is consistent with the peaks location, if $h \leq 0.64$

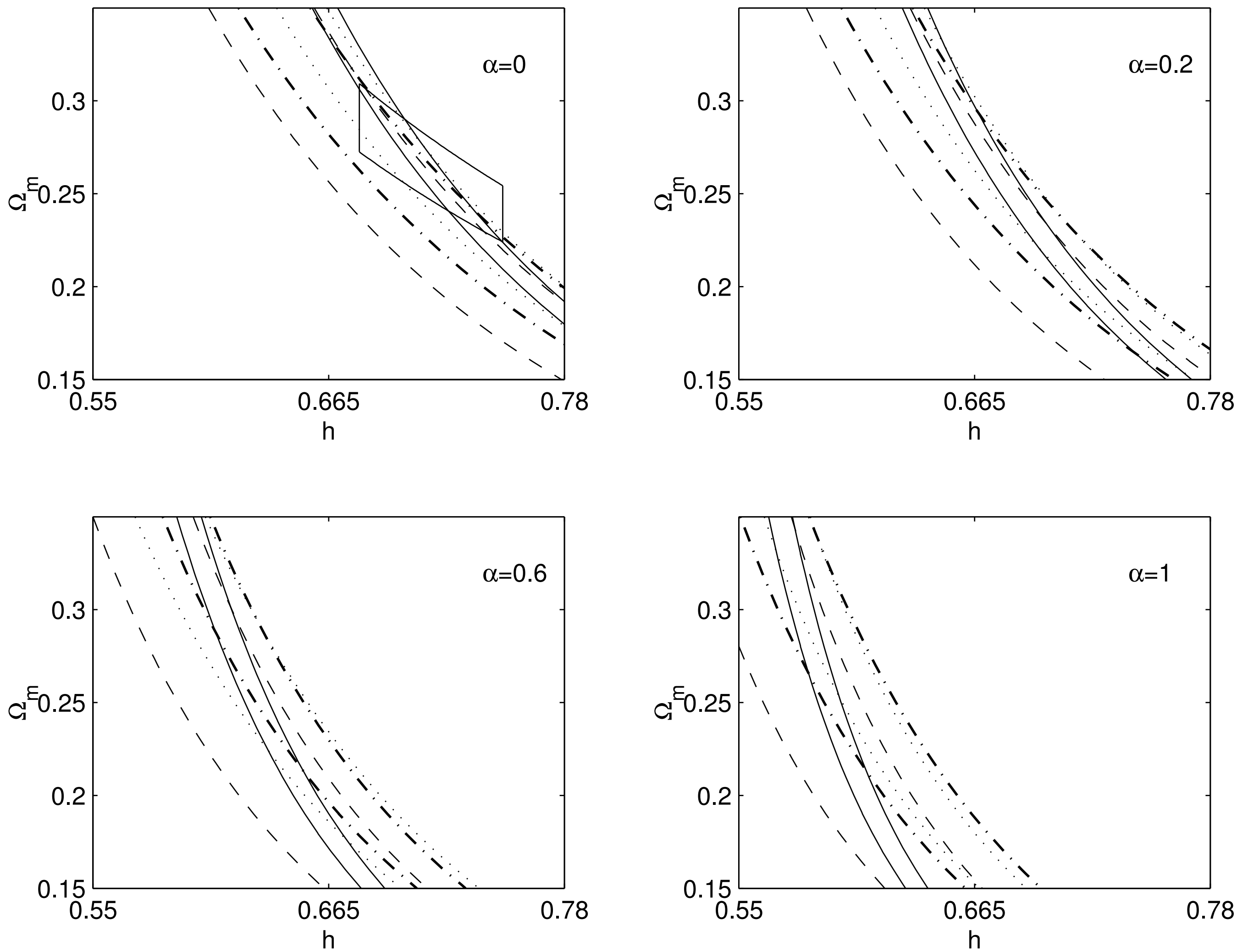

Figure 10: Contour plots of the first three Doppler peaks and first trough locations in the (Ω_m, h) plane for GCG model, with $n_s = 0.97$, for different values of α. Full, dashed, dot-dashed and dotted contours correspond to observational bounds on, respectively, ℓ_{p_1}, ℓ_{p_2}, ℓ_{p_3} and ℓ_{d_1}. The box on the $\alpha = 0$ plot (corresponds to ΛCDM model) indicates the bounds on h and $\Omega_m h^2$ from a combination of WMAP, ACBAR, CBI, “dFGRS and Ly$_\alpha$.

Supernovae Constraints

SNe Ia data sets:

Tonry at al. (2003) 230 points

Barris at al. (2004) 23 points

Riess at al. (2004) - Gold sample (HST) 143 (157) points

- Apparent magnitude:

$$m(z) = \mathcal{M} + 5\log_{10} D_L(z)$$

where $D_L = \frac{H_0}{c} d_L(z)$, $d_L(z) = r(z)(1+z)$ is the luminosity distance and $r(z)$ the comoving distance

$$r(z) = c\int_0^z \frac{dz'}{H(z')}$$

- Absolute magnitude (taken to be constant for all SNe Ia):

$$\mathcal{M} = M + 5\log_{10}\left(\frac{c/H_0}{1\ Mpc}\right) + 25$$

We consider points with $z > 0.01$ and with host galaxy extinction $A_v > 0.5$. This yields 194 points. The Gold and HST data sets were studied in Bento et al., Phys. Rev. D71 (2005) 063501.

- SNe Ia data points are listed in terms of $\log_{10} d_L(z)$ and the error $\sigma_{\log_{10} d_L}(z)$
- The best fit model is obtained by minimizing the quantity

$$\chi^2 = \sum_{i=1}^{194}\left[\frac{\log_{10} d_{L\mathrm{obs}}(z_i) - 0.2\mathcal{M}' - \log_{10} d_{L\mathrm{th}}(z_i; c_\alpha)}{\sigma_{\log_{10} d_L}(z_i)}\right]^2$$

where $\mathcal{M}' = \mathcal{M} - \mathcal{M}_{obs}$ denotes the difference between the actual $\mathcal{M}$ and the assumed value $\mathcal{M}_{obs}$ in the data. Due to the uncertainty arising from the peculiar motion at low redshift one adds $\Delta v = 500$ km s^{-1} to $\sigma^2_{\log_{10} d_L}(z)$

$$\sigma^2_{\log_{10} d_L}(z) \rightarrow \sigma^2_{\log_{10} d_L}(z) + \left(\frac{1}{\ln 10}\frac{1}{D_L}\frac{\Delta v}{c}\right)^2$$

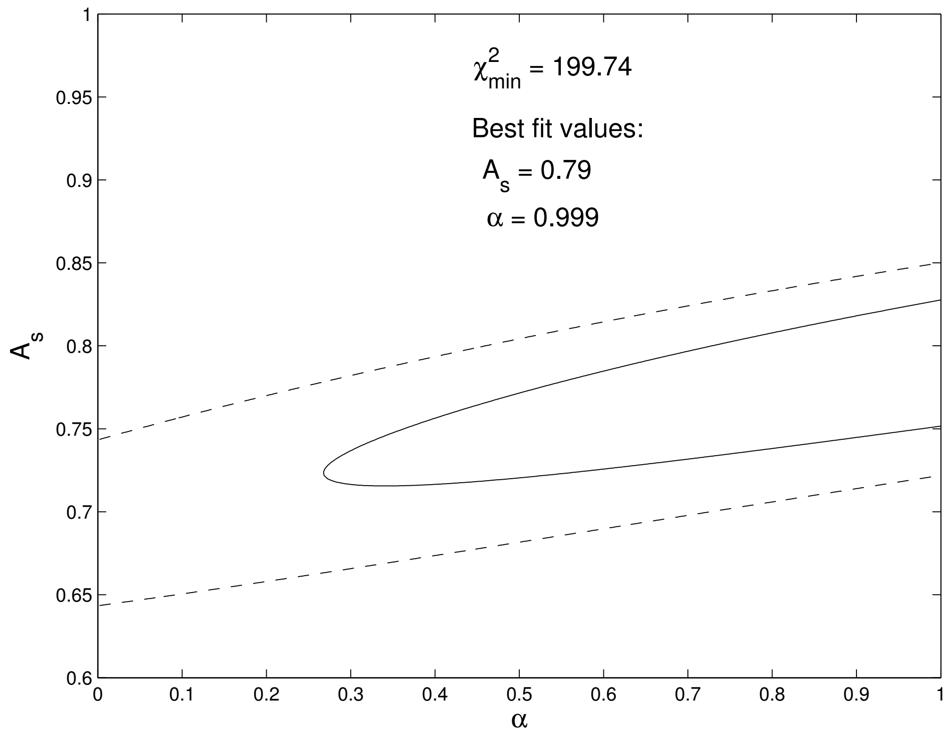

Figure 11: Confidence contours in the $\alpha - A_s$ parameter space for flat unified GCG model. The solid and dashed lines represent the 68% and 95% confidence regions, respectively. The best fit value used for $\mathcal{M}^{'}$ is -0.033.

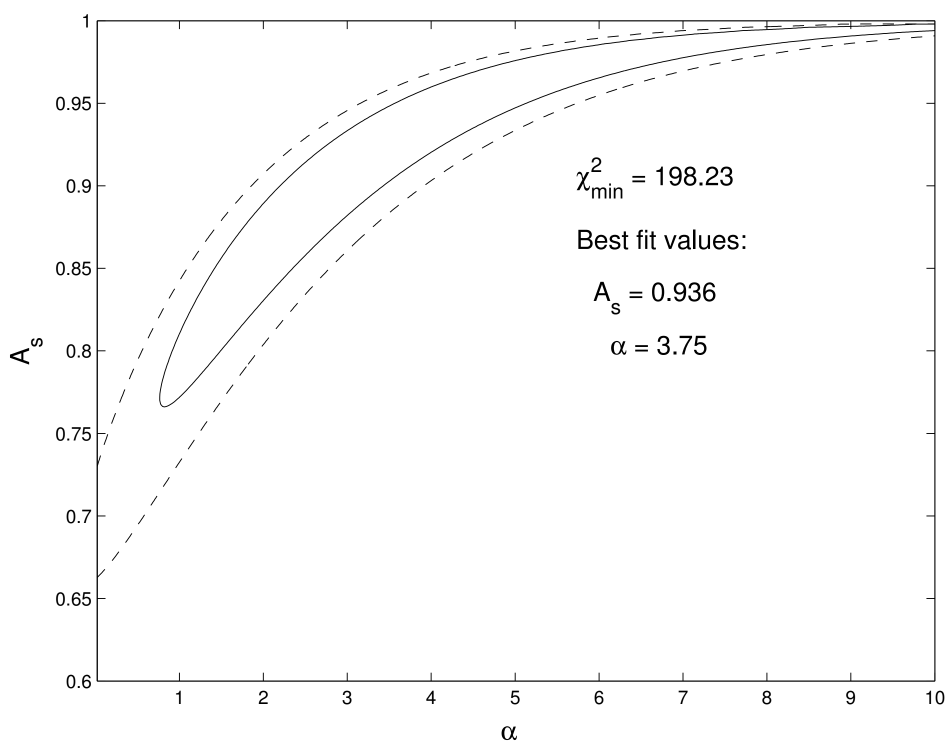

Figure 12: Same as previous Figure, but with a wider range for α.

• Unphysical oscillations or exponential blow-up in the matter power spectrum at present in the unified model?

[Sandvik, Tegmark, Zaldarriaga, Waga 2004]

• Solution: Decompose the energy density into a pressureless dark matter component, ρ_{dm}, and a dark energy component, ρ_X, dropping the phantom component

[M.C. Bento, O. B., A.A. Sen 2004]

Introduce the redshift dependence in the pressure and the energy density ($a_0 = 1$)

$$p_{ch} = -\frac{A}{\left[A + B(1+z)^{3(1+\alpha)}\right]^{\frac{\alpha}{1+\alpha}}}$$

$$\rho_{ch} = \left[A + B(1+z)^{3(1+\alpha)}\right]^{\frac{1}{1+\alpha}}$$

Equation of state:

$$w = \frac{p_{ch}}{\rho_{ch}} = \frac{p_X}{\rho_{dm} + \rho_X} = \frac{w_X \rho_X}{\rho_{dm} + \rho_X} \quad .$$

where

$$\rho_X = -\frac{\rho_{dm}}{1 + w_X \left[1 + \frac{B}{A}(1+z)^{3(1+\alpha)}\right]}$$

As $\rho_X \geq 0$ then $w_X \leq 0$ for early times ($z \gg 1$) and $w_X \leq -1$ for future ($z = -1$). Hence, one concludes that $w_X \leq -1$ for the entire history of the universe. The case $w_X < -1$ corresponds to the so-called phantom-like dark energy, which violates the dominant-energy condition and leads to an ill defined sound velocity. If one excludes this possibility:

$$\rho = \rho_{dm} + \rho_\Lambda$$

where

$$\rho_{dm} = \frac{B(1+z)^{3(1+\alpha)}}{\left[A + B(1+z)^{3(1+\alpha)}\right]^{\frac{\alpha}{1+\alpha}}}$$

$$\rho_\Lambda = -p_\Lambda = \frac{A}{\left[A + B(1+z)^{3(1+\alpha)}\right]^{\frac{\alpha}{1+\alpha}}}$$

from which one obtains the scaling behaviour

$$\frac{\rho_{dm}}{\rho_\Lambda} = \frac{B}{A}(1+z)^{3(1+\alpha)}$$

• The entanglement of dark energy and dark matter is such that the energy exchange, which is described by

$$\dot{\rho}_{dm} + 3H\rho_{dm} = -\dot{\rho}_\Lambda \quad ,$$

implies that the dominance of dark energy at $z \simeq 0.2$ is correlated with the growth of structure!

• The linear perturbation eq. for dark matter in the Newtonian limit:

$$\frac{\partial^2 \delta_{dm}}{\partial t^2} + \left[2\frac{\dot{a}}{a} + \frac{\Psi}{\rho_{dm}}\right]\frac{\partial \delta_{dm}}{\partial t}\left[4\pi G\rho_{dm} - 2\frac{\dot{a}}{a}\frac{\Psi}{\rho_{dm}} - \frac{\partial}{\partial t}\left[\frac{\Psi}{\rho_{dm}}\right]\right]\delta_{dm} = 0$$

where $\Psi = -\frac{1}{8\pi G}\dot{\Lambda}$ and $\Lambda = 8\pi G\rho_\Lambda$. For $\Psi = 0$, i.e. no energy transfer, one recovers the standard equation for the dark matter perturbation in the ΛCDM case.

The study of evolution of δ_{dm} allow obtaining the behaviour of the bias parameter, $b \equiv \delta_b/\delta_{dm}$, of the linear growth function $D(y) \equiv \delta/\delta_0$, where $y = ln(a)$ and of the so-called growth exponent $m(y) = D'(y)/D(y)$

Observational values obtained from the 2DF survey for the bias and the distortion parameter, $\beta \equiv m/b$, in the context of the ΛCDM model

$$\beta = 0.49 \pm 0.09 \quad , \quad b = 1.04 \pm 0.14$$

imply that $m = 0.51 \pm 0.11$ and $\alpha \sim 0.1 - 0.15$.

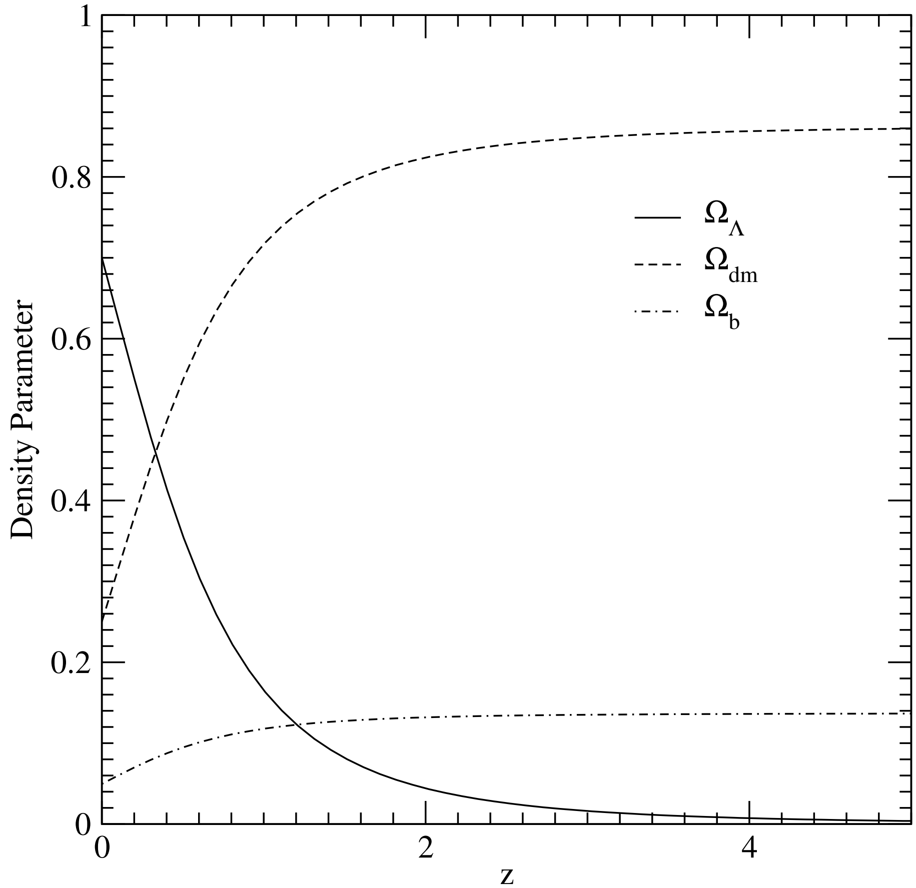

Figure 13: Ω_{dm} and Ω_Λ and Ω_b as a function of redshift. We have assumed $\Omega_{dm0} = .25$, $\Omega_{\Lambda 0} = 0.7$ and $\Omega_{b0} = 0.05$ and $\alpha = 0.2$.

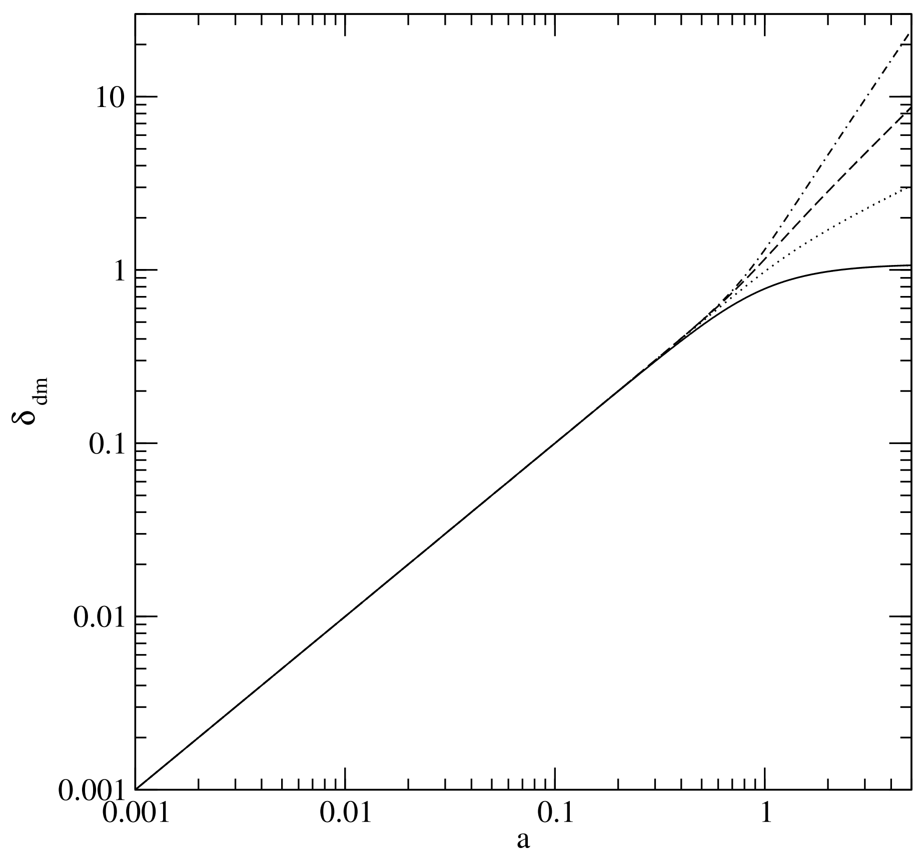

Figure 14: δ_{dm} as function of scale factor. The solid, dotted, dashed and dash-dot lines correspond to $\alpha = 0, 0.2, 0.4, 0.6$, respectively. We have assumed $\Omega_{dm} = 0.25, \Omega_b = 0.05$ and $\Omega_\Lambda = 0.7$.

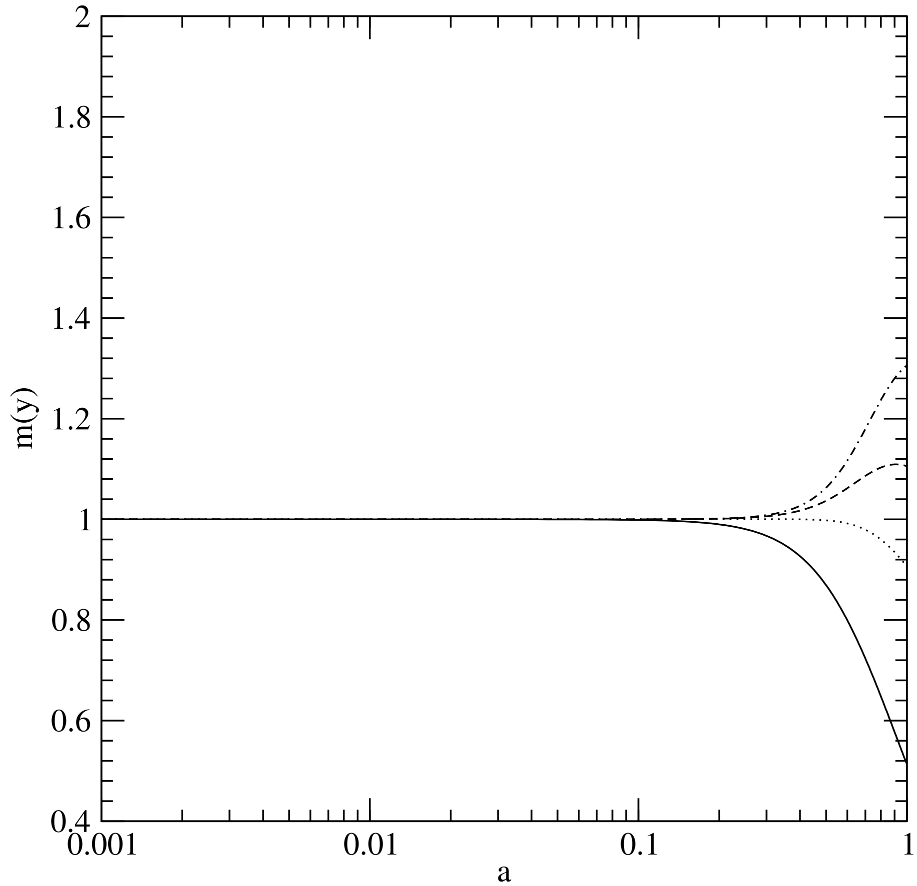

Figure 15: The growth factor $m(y)$ as a function of scale factor a. The solid, dotted, dashed and dash-dot lines correspond to$\alpha = 0, 0.2, 0.4, 0.6$, respectively. We have assumed $\Omega_{dm} = 0.25, \Omega_b = 0.05$ and $\Omega_\Lambda = 0.7$.

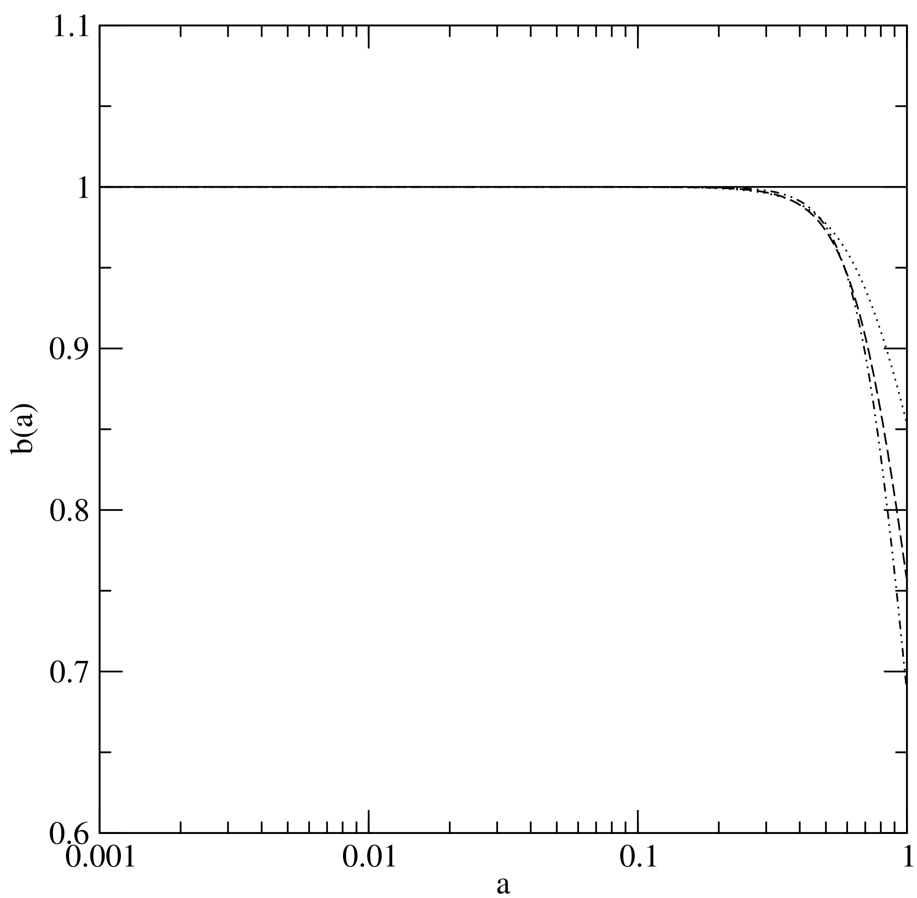

Figure 16: The bias b as a function of the scale factor, a. The solid, dotted, dashed and dash-dot lines correspond to $\alpha = 0, 0.2, 0.4, 0.6$, respectively. We have assumed $\Omega_{dm} = 0.25, \Omega_b = 0.05$ and $\Omega_\Lambda = 0.7$.

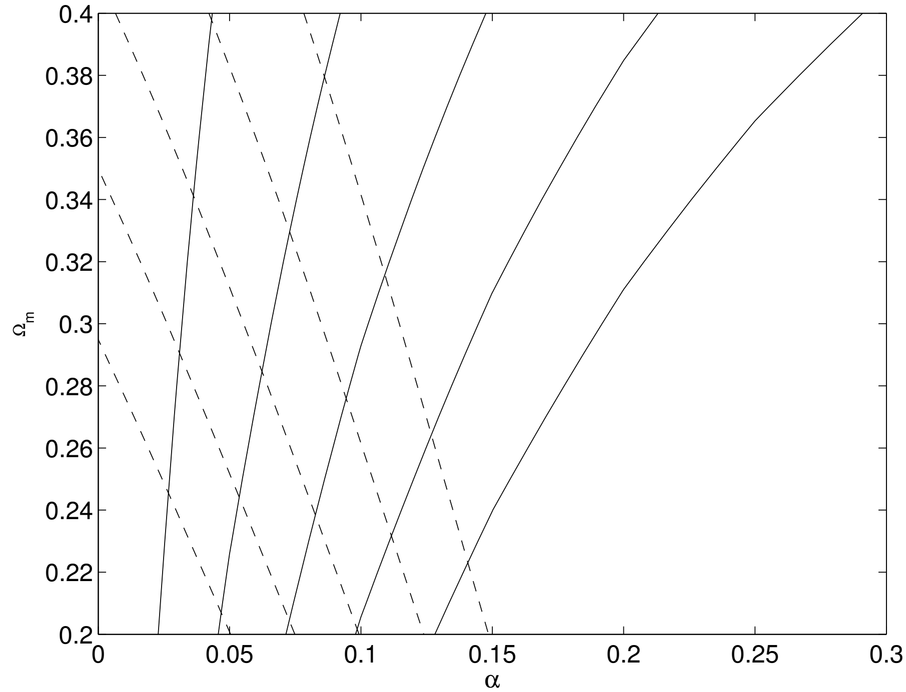

Figure 17: Contours for parameters b and m in the $\Omega_m - \alpha$ plane. Solid lines are for b whereas dashed lines are for m. For b, contour values are $0.98, 0.96, ..., 0.9$ from left to right. For m, contour values are $0.6, 0.65, ..., 0.8$ from left to right.

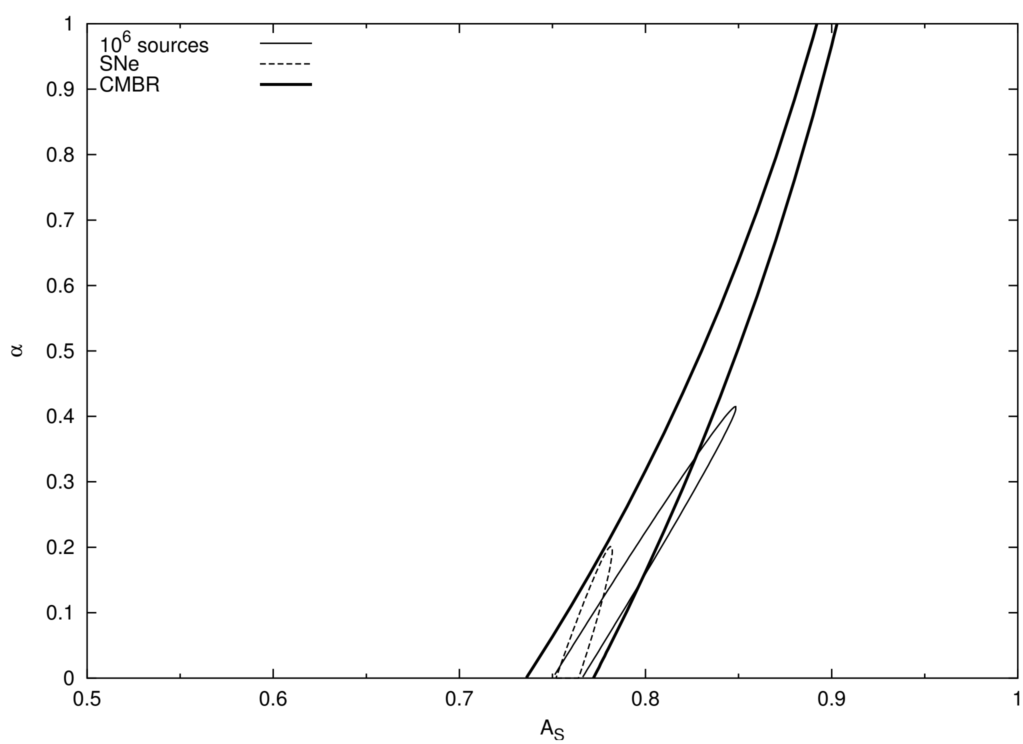

Figure 18: Joint 68% CL confidence regions for Model II using both SNe, gravitational lensing statistics and CMBR constraints.